Chapter 29

Tau Decays

29.1 Hadronic τ Decays

The pure leptonic or semileptonic character of τ decays provides a clean laboratory for performing very precise tests of the electroweak gauge structure at the 0.1% to 1% level. Moreover, hadronic τ decays turn out to be a beautiful laboratory for studying strong interaction effects at low energies [5, 6, 7, 8]. Accurate determinations of the QCD coupling and the strange quark mass have been obtained with τ-decay data. More recently, a very competitive estimate of the quark mixing $|V_{us}|$ has been also extracted from Cabibbo suppressed τ decays.

The excellent experimental conditions offered by the tau-charm factory will allow for further analyses of many aspects of τ physics with low systematics. The BEPCII collider could produce large statistical samples as many as 50 million $\tau^+\tau^-$ pairs per year, providing the opportunity for an extensive programme of high-precision measurements with τ leptons. The B-factories have already produced much larger data samples, which will be further increased at LHC and, if approved, at future Super-B factories. However, the threshold region makes possible a much better control of backgrounds and systematic errors for a number of measurements. Thus, the tau-charm factory combines the optimum conditions to perform a number of very accurate measurements.

29.1.1 A Laboratory for QCD[1]

The inclusive character of the total τ hadronic width renders possible an accurate calculation of the ratio [(γ) represents additional photons or lepton pairs]

$$R_\tau \equiv \frac{\Gamma[\tau^- \to \nu_\tau \,\text{hadrons}\,(\gamma)]}{\Gamma[\tau^- \to \nu_\tau e^- \bar{\nu}_e(\gamma)]} \;=\; R_{\tau,V} + R_{\tau,A} + R_{\tau,S}\,, \tag{29.1.1}$$

using analyticity constraints and the Operator Product Expansion [9, 10, 11, 12, 13]. One can separately compute the contributions associated with specific quark currents. $R_{\tau,V}$ and $R_{\tau,A}$ correspond to the Cabibbo–allowed decays through the vector and axial-vector currents, while $R_{\tau,S}$ contains the remaining Cabibbo–suppressed contributions.

[1] By Antonio Pich

The theoretical prediction for $R_{\tau,V+A}$ can be expressed as [11]

$$R_{\tau,V+A} = N_C \, |V_{ud}|^2 \, S_{\rm EW} \, \{1 + \delta_{\rm P} + \delta_{\rm NP}\} \, , \tag{29.1.2}$$

where $N_C = 3$ denotes the number of quark colours and $S_{\rm EW} = 1.0201 \pm 0.0003$ contains the electroweak radiative corrections [14]. The dominant correction ($\sim 20\%$) is the perturbative QCD contribution $\delta_{\rm P}$, which is fully known to $O(\alpha_s^3)$ [11] and includes a resummation of the most important higher-order effects [12].

Non-perturbative contributions are suppressed by six powers of the τ mass [11] and, therefore, are very small. Their numerical size has been determined from the invariant–mass distribution of the final hadrons in τ decay, through the study of weighted integrals that can be calculated theoretically in the same way as R_τ [15]:

$$R_\tau^{kl} \equiv \int_0^{m_\tau^2} ds \, \left(1 - \frac{s}{m_\tau^2}\right)^k \, \left(\frac{s}{m_\tau^2}\right)^l \, \frac{dR_\tau}{ds} \, . \tag{29.1.3}$$

The predicted suppression [11] of the non-perturbative corrections has been confirmed by ALEPH [16], CLEO [17] and OPAL [18]. The most recent analysis [16] gives

$$\delta_{\rm NP} \; = \; -0.0043 \pm 0.0019 \, . \tag{29.1.4}$$

The QCD prediction for $R_{\tau,V+A}$ is then completely dominated by the perturbative contribution; non-perturbative effects being smaller than the perturbative uncertainties from uncalculated higher-order corrections. The result turns out to be very sensitive to the value of $\alpha_s(m_\tau^2)$, thereby allowing for an accurate determination of the fundamental QCD coupling [10, 11]. The experimental measurement $R_{\tau,V+A} = 3.471 \pm 0.011$ implies [19]

$$\alpha_s(m_\tau^2) = 0.345 \pm 0.004_{\rm exp} \pm 0.009_{\rm th} \, . \tag{29.1.5}$$

The strong coupling measured at the τ mass scale is significantly larger than the values obtained at higher energies. From the hadronic decays of the Z, one gets $\alpha_s(M_Z^2) = 0.1186 \pm 0.0027$ [20], which differs from the τ decay measurement by more than twenty standard deviations. After evolution up to the scale M_Z [21], the strong coupling constant in Eq. 29.1.5 decreases to [19]

$$\alpha_s(M_Z^2) = 0.1215 \pm 0.0012 \, , \tag{29.1.6}$$

in excellent agreement with the direct measurements at the Z peak and with a similar accuracy. The comparison of these two determinations of α_s in two extreme energy regimes, m_τ and M_Z, provides a beautiful test of the predicted running of the QCD coupling; *i.e.*, a very significant experimental verification of *asymptotic freedom*.

With $\alpha_s(m_\tau^2)$ fixed to the value in Eq. 29.1.5, the same theoretical framework gives definite predictions for the semi-inclusive τ decay widths $R_{\tau,V}$, $R_{\tau,A}$ and $R_{\tau,S}$, in good agreement with the experimental measurements. Moreover, using the measured invariant mass distributions, one can study (for each separate V, A and S component) the integrated moments defined in Eq. 29.1.3, with arbitrary weight functions and/or varying the upper end of integration in the range $s_0 \leq m_\tau^2$. This allows one to investigate many non-perturbative aspects of the strong interactions [22]. For instance, $R_{\tau,V} - R_{\tau,A}$ is a pure non-perturbative quantity; basic QCD properties force the associated mass distribution to obey

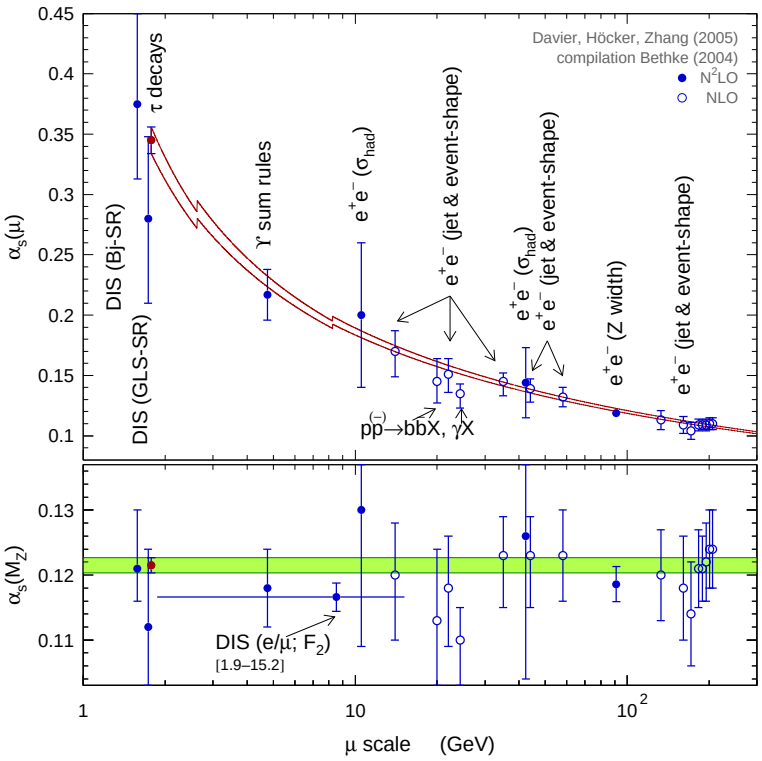

Figure 29.1: Measured values of α_s at different scales. The curves show the energy dependence predicted by QCD, using $\alpha_s(m_\tau^2)$ as input. The corresponding extrapolated $\alpha_s(M_Z^2)$ values are shown at the bottom, where the shaded band displays the τ decay result [19].

a series of chiral sum rules [22, 23], which relate the τ measurements with low-energy non-perturbative observables such as the pion decay constant f_π or the electromagnetic pion mass difference $m_{\pi^\pm} - m_{\pi^0}$. One can also extract the non-perturbative contributions to the OPE of the QCD vector and axial-vector current correlators. The determination of these effects is needed to perform many theoretical predictions of other important observables, such as, for instance, the kaon CP-violating ratio ε'/ε. The measured vector spectral distribution can also be used to estimate the hadronic vacuum polarization contribution to $\alpha(M_Z)$ and to the muon anomalous magnetic moment.

29.1.2 Determinations of m_s and V_{us} in Hadronic τ Decays[2]

Separate measurements of the $|\Delta S| = 0$ and $|\Delta S| = 1$ τ decay widths will allow us to pin down the $SU(3)_{fl}$ breaking effects induced by the strange quark mass [24, 25, 26, 27, 28, 29, 30], through the differences [25]

$$\delta R_\tau^{kl} \equiv \frac{R_{\tau,V+A}^{kl}}{|V_{ud}|^2} - \frac{R_{\tau,S}^{kl}}{|V_{us}|^2} \approx 24\,\frac{m_s^2(m_\tau^2)}{m_\tau^2}\,\Delta_{kl}(\alpha_s) - 48\pi^2\,\frac{\delta O_4}{m_\tau^4}\,Q_{kl}(\alpha_s)\,. \qquad (29.1.7)$$

The perturbative QCD corrections $\Delta_{kl}(\alpha_s)$ and $Q_{kl}(\alpha_s)$ are known to $O(\alpha_s^3)$ and $O(\alpha_s^2)$, respectively [25, 30]. Since the longitudinal contribution to $\Delta_{kl}(\alpha_s)$ does not converge well,

[2]By A. Pich

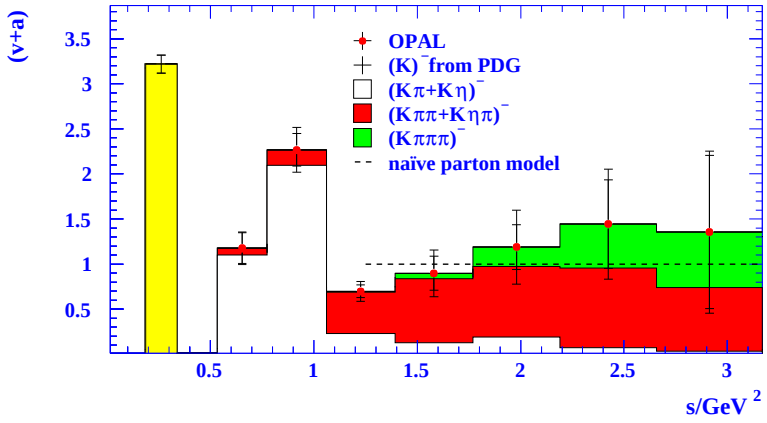

Figure 29.2: The OPAL measurement of the spectral distribution in $|\Delta S| = 1$ τ decays [32].

the $J = 0$ QCD expression is replaced by its corresponding phenomenological hadronic parametrization [29], which is much more precise because it is strongly dominated by the well known kaon pole. The small non-perturbative contribution, $\delta O_4 \equiv \langle 0|m_s\bar{s}s - m_d\bar{d}d|0\rangle = -(1.5\pm0.4)\times10^{-3}$ GeV^4, has been estimated with Chiral Perturbation Theory techniques [25].

From the measured moments δR_τ^{k0} $(k = 0, 1, 2, 3, 4)$ [31, 32], it is possible to determine the strange quark mass; however, the extracted value depends sensitively on the modulus of the Cabibbo–Kobayashi–Maskawa matrix element $|V_{us}|$. It appears, then, more natural to turn things around and, with an input for m_s obtained from other sources, determine $|V_{us}|$ [29]. The most sensitive moment is δR_τ^{00}:

$$|V_{us}|^2 = \frac{R_{\tau,S}^{(0,0)}}{\frac{R_{\tau,V+A}^{(0,0)}}{|V_{ud}|^2} - \delta R_{\tau,\mathrm{th}}^{(0,0)}} \,. \tag{29.1.8}$$

Using $m_s(2\ \mathrm{GeV}) = (94 \pm 6)$ MeV, which includes the most recent determinations of m_s from lattice and QCD Sum Rules [33], one obtains $\delta R_{\tau,\mathrm{th}}^{00} = 0.240 \pm 0.032$ [29]. This prediction is much smaller than $R_{\tau,V+A}^{(0,0)}/|V_{ud}|^2$, making the theoretical uncertainty in Eq. 29.1.8 negligible in comparison with the experimental inputs $R_{\tau,V+A}^{(0,0)} = 3.471 \pm 0.011$ and $R_{\tau,S}^{(0,0)} = 0.1686 \pm 0.0047$ [19]. Taking $|V_{ud}| = 0.97377 \pm 0.00027$ [2], one gets [29]

$$|V_{us}| = 0.2220 \pm 0.0031_{\mathrm{exp}} \pm 0.0011_{\mathrm{th}} \,. \tag{29.1.9}$$

This result is competitive with the standard K_{e3} determination, $|V_{us}| = 0.2234 \pm 0.0024$ [34]. The precision should be considerably improved in the near future because the error is dominated by the experimental uncertainty, which can be reduced with the much better data samples from BaBar, Belle and *BES-III*. Thus, τ data has the potential to provide the best determination of $|V_{us}|$.

With future high-precision τ data, a simultaneous fit of m_s and $|V_{us}|$ should also become possible. A better understanding of the perturbative QCD corrections $\Delta_{kl}(\alpha_s)$ would be very helpful to improve the precision on m_s [28, 29].

29.1.3 Tau Hadronic Spectral Functions[3]

Hadronic tau decays give unique possibilities for performing detailed investigations of hadronic production from the QCD vacuum through the determination of *spectral functions*. Spectral functions play an important role in the understanding of hadron dynamics in the intermediate energy range and provide the basic input for QCD studies and for calculation of the low-energy contributions from the hadronic vacuum polarization.

Definition

The spectral function $v_1(a_1, a_0)$, where subscript refers to the spin of hadronic system, is defined for a non-strange ($\Delta S = 0$) or strange ($\Delta S = 1$) vector (axial-vector) tau decay channel $V^-\nu_\tau$ ($A^-\nu_\tau$), and is obtained by dividing the invariant mass-squared distribution $(1/N_{V/A})(dN_{V/A}/ds)$ by the appropriate kinematic factor and is normalized by the ratio of vector/axial vector branching fraction $\mathcal{B}(\tau \to V^-/A^-\nu_\tau)$ to the branching fraction of the decay to a massless lepton (electron) :.

$$v_1/a_1 = \frac{m_\tau^2}{6|V_{CKM}|^2 S_{EW}} \frac{\mathcal{B}(\tau \to V^-/A^-\nu_\tau)}{\mathcal{B}(\tau \to e^-\nu_e\nu_\tau)} \frac{dN_{V/A}}{N_{V/A}ds} \left[\left(1 - \frac{s}{m_\tau^2}\right)^2 \left(1 + \frac{2s}{m_\tau^2}\right)\right]^{-1}, \tag{29.1.10}$$

$$a_0 = \frac{m_\tau^2}{6|V_{CKM}|^2 S_{EW}} \frac{\mathcal{B}(\tau \to \pi^-\nu_\tau)}{\mathcal{B}(\tau \to e^-\nu_e\nu_\tau)} \frac{dN_A}{N_A ds} \left(1 - \frac{s}{m_\tau^2}\right)^{-2}. \tag{29.1.11}$$

Here S_{EW} is the electroweak radiative correction factor that is introduced in the previous section. Due to the conserved vector current (CVC), there is no $J = 0$ contribution to the vector spectral function; the only contribution to a_0 is assumed to be from the pion pole, with $dN_A/N_A ds = \delta(s - m_\pi^2)$.

Using unitarity and analyticity, the spectral functions are connected to the imaginary parts of the two-point correlation (hadronic vacuum polarization) functions [35, 36]

$$\begin{aligned} \Pi^\mu_{i,j,U}(q^2) &\equiv \int d^4x e^{iqx} \langle 0|T(U^\mu_{ij}(x) U^\mu_{ij}(0)^+)|0\rangle \\ &= (-g^{\mu\nu}q^2 + q^\mu q^\nu)\Pi^{(1)}_{ij,U}(q^2) + q^\mu q^\nu \Pi^{(0)}_{ij,U}(q^2), \end{aligned} \tag{29.1.12}$$

of vector($U^{\mu\nu}_{ij} = V^\nu_{ij} = \overline{q}_j\gamma^\mu q_i$) or axial-vector ($U^\mu_{ij} = V^\mu_{ij} = \overline{q}_j\gamma^\mu\gamma_5 q_i$) quark currents for time-like momenta-squared $q^2 > 0$. The polarization functions $\Pi^{\mu\nu}_{i,j,U}(s)$ have a branch cut along the real axis in the complex $s = q^2$ plane. Their imaginary parts give the spectral functions defined in Eq. 29.1.10. For non-strange currents:

$$\begin{aligned} Im\Pi^{(1)}_{\overline{u}d,V/A}(s) &= \frac{1}{2\pi} v_1/a_1(s), \\ Im\Pi^{(0)}_{\overline{u}d,A}(s) &= \frac{1}{2\pi} v_1/a_0(s). \end{aligned} \tag{29.1.13}$$

[3]By I. Boyko and D. Dedovich

Analytic functions $\Pi^{(J)}ij,U(q^2)$ obey the dispersion relation

$$\Pi^{(J)}ij,U(q^2) = \frac{1}{\pi}\int_0^\infty ds \frac{Im\Pi^{(J)}_{ij,U}(s)}{s-q^2-i\epsilon}. \tag{29.1.14}$$

This dispersion relation allows one to connect the experimentally accessible spectral functions to the correlation functions $\Pi^{(J)}ij,U(q^2)$, which can be derived from QCD theory and are used for theoretical calculations of total cross sections and decay widths.

Tau spectral functions and electron-positron annihilation data

In the limit of isospin invariance, the vector current is conserved (CVC), so that the spectral function for a vector τ decay mode $X^-\nu_\tau$ in a given isospin state for the hadronic system is related to the e^+e^- annihilation cross section of the corresponding isovector final state X^0 :

$$\sigma^{I=1}_{e^+e^-\to X^0}(s) \;=\; \frac{4\pi\alpha^2}{s}\, v_{1,\,X^-}(s)\;, \tag{29.1.15}$$

where α is the electromagnetic fine structure constant. In reality, isospin symmetry is broken, particularly due to electromagnetic effects, and corrections must be applied to compare (and combine) τ-decay and e^+e^- data. A more complete review and further references about sources and value of the symmetry breaking can be found in Refs. [37, 38]. A comparison of two-pion spectral functions obtained from tau decays and e^+e^- data is shown in Fig. 29.3, which is taken from Ref. [38]. Here it is evident that, although the absolute difference is relatively small, there is a clear discrepancy between data, especially above the ρ peak. Another, more "quantitative" way to compare spectral functions is to use e^+e^- data to calculate hadronic tau branching fractions. For the most studied decay, $\tau \to \nu_\tau\pi\pi^0$, different authors [37, 38, 39] give $\tau - e^+e^-$ discrepancies in the range $2.9\sigma - 4.5\sigma$ with differences depending mainly on which e^+e^- data are included in the analysis, while in all cases the τ-decay data are dominated by the ALEPH results. In a recent work [40], a new calculation of isospin breaking corrections is presented, and this reduces the discrepancies mentioned above to 2.6σ and substantially improves the agreement between the shapes of spectral functions obtained from τ-decay and e^+e^- annihilation. Nevertheless, the situation is still far from the "good agreement" state. In addition, the predicted value for the anomalous muon magnetic moment g_μ-2 calculated using combined the τ and e^+e^- data is now 3.6σ away from the most precise measurement. Thus, we now face a very intriguing situation: differences between predictions and measurements are substantial on one side, but still too small to be a sign of new physics on the other side; new reliable measurements will be very useful.

Measurement of Tau Hadronic Spectral Functions at *BES-III*

Experimental tau physics data can be divided into two main groups: Data produced at LEP have low background and high selection efficiency, but are statistically limited. Data from B-factories have almost unlimited statistics, but much worse background conditions due to relatively low multiplicity of hadronic events and the high ratio of the inclusive hadron and the tau-pair production cross-sections. The *BES-III* experiment has

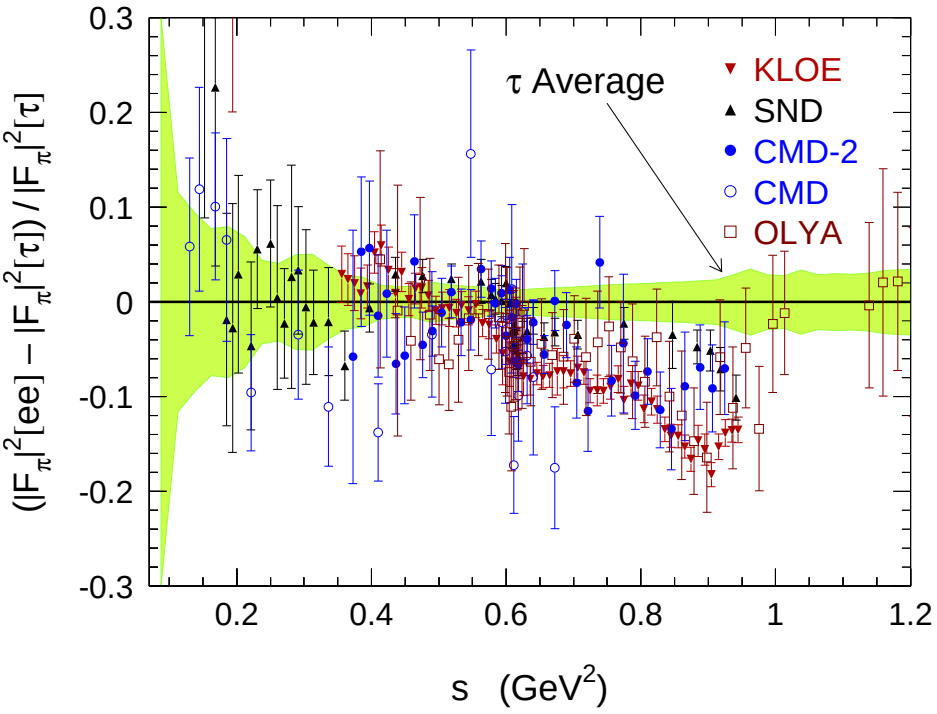

Figure 29.3: Relative comparison of the isospin-breaking-corrected τ data (world average) and $\pi^+\pi^-$ spectral function from e^+e^- annihilation, expressed as a ratio to the τ spectral function. The shaded band gives the uncertainty on the τ spectral function.

no advantage over the B-factories when working at the charmonium resonances. On the other hand, a dedicated "tau" run at an energy slightly below the $\psi(2S)$ resonance would allow a combination of high statistics and excellent background conditions. Using leptonic τ-decay tagging in combination with the usual kinematic selection criteria (high missing momenta, acollinearity and acomplanarity, broken P_t balance) will make it is possible to select an extremely clean sample of τ decays, with backgrounds well below 1%. Another obvious advantage of using lepton-tagged events is that that the selection (in)efficiency causes no bias in the measured values, and only affects the available statistics. Thus, if more strict selection criteria are used, we can say that "we are buying low systematics with statistics." The table below gives a comparison of *BES-III* and ALEPH experimental conditions for τ hadronic branching measurements and spectral functions determinations. The *BES-III* values are computed assuming a three-month dedicated tau run and an 80% tagging efficiency.

	ALEPH	***BES-III***
τ-decays selected	$\sim$ 327000	1.6×10^6
$\tau \to \pi\pi_0\nu_\tau$ decays selected	$\sim$ 81000	$\sim$ 280 000
external background	1.2%	$< 1\%$
hadronic mass reconstruction accuracy	$\sim$ 80 MeV	< 50 MeV

Another very important consideration is the neutral hadron (π^0 most of all) identifi-

cation efficiency. A preliminary simulation shows that the single π^0 registration efficiency for the *BES-III* detector will be about 95% for decays that are within the acceptance of the calorimeter, which is at least as good as that for ALEPH. It should be noted that the tau leptons in LEP events are highly boosted and this results in a large number of merged or overlapped clusters in electromagnetic calorimeters, which require a very complicated (and, therefore, vulnerable to error) analysis. At *BES-III*, the τ decay products are distributed almost uniformly throughout the deector. The main contribution to the neutral pion reconstruction inefficiency will be due to the geometrical acceptance (95%), which can be calculated with high accuracy and should not result in a substantial systematic error. Another attractive possibility is related to the determination of strange spectral functions. At LEP experiments, kaons were identified only on a statistical basis. At *BES-III*, kaons produced in tau decay will have momenta below 0.8 GeV/c, *i.e.* in the momentum range where they can be selected with high purity by the TOF and dE/dX measurements.

Thus, a three-month dedicated tau run at *BES-III* has a good chance of providing the most accurate measurements of the hadronic spectral functions.

29.2 Leptonic Tau decays

The precise measurement of the different exclusive τ decays provides very valuable information to test the Standard Model, both in the electroweak and strong sectors. The threshold region, with its kinematical advantages and low backgrounds, makes accurate studies of the lowest-multiplicity decay modes possible.

29.2.1 Leptonic Decays and Universality Tests[4]

The leptonic decays $\tau^- \to l^- \bar{\nu}_l \nu_\tau$ $(l = e, \mu)$ are theoretically understood at the level of the electroweak radiative corrections. Within the Standard Model

$$\Gamma_{\tau\to l} \equiv \Gamma(\tau^- \to \nu_\tau l^- \bar{\nu}_l) = \frac{G_F^2 m_\tau^5}{192\pi^3} f\left(\frac{m_l^2}{m_\tau^2}\right) r_{EW}, \tag{29.2.16}$$

where $f(x) = 1 - 8x + 8x^3 - x^4 - 12x^2 \log x$. The factor r_{EW} takes into account radiative corrections not included in the Fermi coupling constant G_F, and the non-local structure of the W propagator [14]; these effects are quite small [$\alpha(m_\tau) = 1/133.3$]:

$$r_{EW} = \left[1 + \frac{\alpha(m_\tau)}{2\pi}\left(\frac{25}{4} - \pi^2\right)\right]\left[1 + \frac{3}{5}\frac{m_\tau^2}{M_W^2} - 2\frac{m_l^2}{M_W^2}\right] = 0.9960\,. \tag{29.2.17}$$

Using the value of G_F measured in μ decay in Eq. (29.2.16), yields a relation between the τ lifetime and the leptonic branching ratios:

$$B_{\tau\to e} \equiv \mathrm{Br}(\tau^- \to e^- \bar{\nu}_e \nu_\tau) = \frac{B_{\tau\to\mu}}{0.972564 \pm 0.000010} = \frac{\tau_\tau}{(1632.1 \pm 1.4) \times 10^{-15}\,\mathrm{s}}\,. \tag{29.2.18}$$

Here the quoted errors reflect the present uncertainty of 0.3 MeV in the value of m_τ.

[4] A. Pich

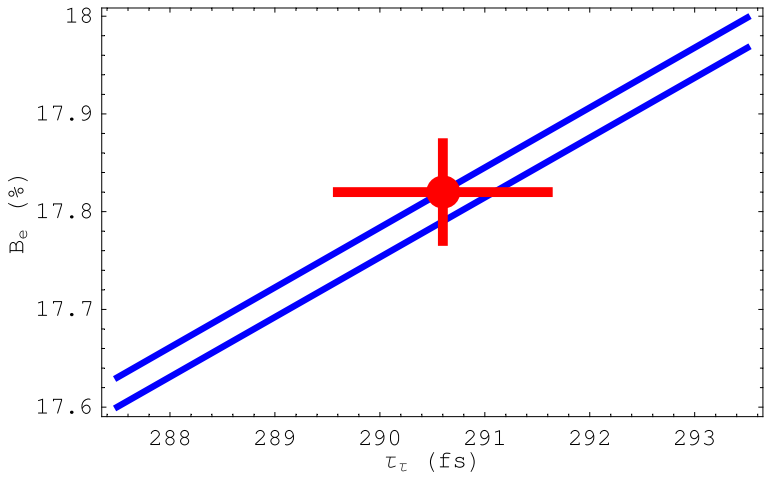

Figure 29.4: The relation between $B_{\tau\to e}$ and τ_τ. The diagonal band corresponds to Eq. (29.2.18).

Table 29.1: Present constraints on $|g_l/g_{l'}|$ [7, 34].

	$B_{\tau\to e}\,\tau_\mu/\tau_\tau$	$\Gamma_{\tau\to\pi}/\Gamma_{\pi\to\mu}$	$\Gamma_{\tau\to K}/\Gamma_{K\to\mu}$	$B_{W\to\tau}/B_{W\to\mu}$
$\lvert g_\tau/g_\mu\rvert$	1.0004 ± 0.0022	0.996 ± 0.005	0.979 ± 0.017	1.039 ± 0.013
	$B_{\tau\to\mu}/B_{\tau\to e}$	$B_{\pi\to\mu}/B_{\pi\to e}$	$B_{K\to\mu}/B_{K\to e}$	$B_{K\to\pi\mu}/B_{K\to\pi e}$
$\lvert g_\mu/g_e\rvert$	1.0000 ± 0.0020	1.0017 ± 0.0015	1.012 ± 0.009	1.0002 ± 0.0026
	$B_{W\to\mu}/B_{W\to e}$		$B_{\tau\to\mu}\,\tau_\mu/\tau_\tau$	$B_{W\to\tau}/B_{W\to e}$
$\lvert g_\mu/g_e\rvert$	0.997 ± 0.010	$\lvert g_\tau/g_e\rvert$	1.0004 ± 0.0023	1.036 ± 0.014

The predicted value of $B_{\tau\to\mu}/B_{\tau\to e}$ is in excellent agreement with the measured ratio $B_{\tau\to\mu}/B_{\tau\to e} = 0.9725 \pm 0.0039$. As shown in Fig. 29.4, the relation between $B_{\tau\to e}$ and τ_τ is also well satisfied by the present data. Note that this relation is very sensitive to the value of the τ mass [$\Gamma_{\tau\to l} \propto m_\tau^5$].

These measurements can be used to test the universality of the W couplings to the leptonic charged currents, *i.e.* $g_e = g_\mu = g_\tau \equiv g$. The $B_{\tau\to\mu}/B_{\tau\to e}$ ratio constraints $|g_\mu/g_e|$, while the $B_{\tau\to e}/\tau_\tau$ relation provides information on $|g_\tau/g_\mu|$. As shown in Table 29.1, the present data verify the universality of the leptonic charged-current couplings to the 0.2% level.[5]

The τ leptonic branching fractions and the τ lifetime are known with a precision of 0.3%. Slightly improved lifetime measurements are expected from BaBar and Belle. For comparison, the μ lifetime is known with an accuracy of 10^{-5}, which should be further improved to 10^{-6} by the MuLan experiment at PSI [41].

Universality tests also require a precise determination of m_τ^5, which is only known to the 0.08% level. Two new preliminary measurements of the τ mass have been presented

[5] Br($W \to \nu_\tau\tau$) is $2.1\,\sigma/2.7\,\sigma$ larger than Br($W \to \nu_e e/\nu_\mu\mu$). The stringent limits on $|g_\tau/g_{e,\mu}|$ from W-mediated decays makes it unlikely that this is a real physical effect.

recently:

$$m_\tau = \begin{cases} 1776.71 \pm 0.13 \pm 0.35 \text{ MeV} & \text{[Belle]}, \\ 1776.80\,^{+0.25}_{-0.23} \pm 0.15 \text{ MeV} & \text{[KEDR]}. \end{cases} \tag{29.2.19}$$

The Belle value [42] is based on a pseudomass analysis of $\tau \to \nu_\tau 3\pi$ decays, while the KEDR result [43] comes from a measurement of $\tau^+\tau^-$ threshold production, taking advantage of a precise energy calibration through the resonance depolarization method. In both cases the achieved precision is getting close to the present BES-I dominated value, $m_\tau = 1776.99\,^{+0.29}_{-0.26}$ [2]. KEDR aims to obtain a final accuracy of 0.15 MeV. A precision of better than 0.1 MeV should be easily achieved at *BES-III* [44], through a detailed analysis of $\sigma(e^+e^- \to \tau^+\tau^-)$ at threshold [1, 45, 46], as discussed in detail in Chapt. 30.

29.2.2 Lorentz Structure[6]

With high statistics, the leptonic τ decay modes provide opportnities to investigate the Lorentz structure of the decay amplitude, through the analysis of the energy and angular distribution of the final charged lepton. The most general, local, derivative-free, lepton-number conserving, four-lepton interaction Hamiltonian, consistent with locality and Lorentz invariance [47, 48, 49, 50],

$$\mathcal{H} \,=\, 4\,\frac{G_{l'l}}{\sqrt{2}} \sum_{n,\epsilon,\omega} g^n_{\epsilon\omega} \left[\overline{l'_\epsilon}\Gamma^n(\nu_{l'})_\sigma\right] \left[\overline{(\nu_l)_\lambda}\Gamma_n l_\omega\right] , \tag{29.2.20}$$

contains ten complex coupling constants or, since a common phase is arbitrary, nineteen independent real parameters that could be different for each leptonic decay. The sub-indices $\epsilon, \omega, \sigma, \lambda$ label the chiralities (left-handed, right-handed) of the corresponding fermions, and n the type of interaction: scalar (I), vector (γ^μ) and tensor ($\sigma^{\mu\nu}/\sqrt{2}$). For given n, ϵ, ω, the neutrino chiralities σ and λ are uniquely determined.

Taking out a common factor $G_{l'l}$, which is determined by the total decay rate, the coupling constants $g^n_{\epsilon\omega}$ are normalized to [49]

$$\begin{aligned} 1 = \frac{1}{4}\,&\left(|g^S_{RR}|^2 + |g^S_{RL}|^2 + |g^S_{LR}|^2 + |g^S_{LL}|^2\right) \,+\, 3\,\left(|g^T_{RL}|^2 + |g^T_{LR}|^2\right) \\ &+ \left(|g^V_{RR}|^2 + |g^V_{RL}|^2 + |g^V_{LR}|^2 + |g^V_{LL}|^2\right) . \end{aligned} \tag{29.2.21}$$

In the Standard Model, $g^V_{LL} = 1$ and all the other $g^n_{\epsilon\omega} = 0$. The sums of all contributions in Eq. 29.2.21 with identical initial and final chiralities, $\mathcal{Q}_{\epsilon\omega}$, can be interpreted as the probabilities for the decay of an ω-handed l^- into an ϵ-handed daughter lepton. Upper bounds on any of these (positive-semidefinite) probabilities translate into corresponding limits for all couplings with the given chiralities. The measurement of the τ polarization is possible due to the fact that the spins of the $\tau^+\tau^-$ pair produced in e^+e^- annihilation are strongly correlated. Table 29.2 shows the present 90% C.L. experimental bounds on the $g^n_{\epsilon\omega}$ couplings.

[6] By A. Pich

Table 29.2: 90% C.L. experimental bounds [2] for the normalized τ-decay couplings $g'^n_{\epsilon\omega} \equiv g^n_{\epsilon\omega}/N^n$, where $N^n \equiv \max(|g^n_{\epsilon\omega}|) = 2,\ 1,\ 1/\sqrt{3}$ for $n =$ S, V, T.

$\tau^- \to e^-\bar{\nu}_e\nu_\tau$			
$\lvert g^S_{RR}\rvert < 0.70$	$\lvert g^S_{LR}\rvert < 0.99$	$\lvert g^S_{RL}\rvert < 2.01$	$\lvert g^S_{LL}\rvert < 2.01$
$\lvert g^V_{RR}\rvert < 0.17$	$\lvert g^V_{LR}\rvert < 0.13$	$\lvert g^V_{RL}\rvert < 0.52$	$\lvert g^V_{LL}\rvert < 1.01$
$\lvert g^T_{RR}\rvert \equiv 0$	$\lvert g^T_{LR}\rvert < 0.08$	$\lvert g^T_{RL}\rvert < 0.51$	$\lvert g^T_{LL}\rvert \equiv 0$
$\tau^- \to \mu^-\bar{\nu}_\mu\nu_\tau$			
$\lvert g^S_{RR}\rvert < 0.72$	$\lvert g^S_{LR}\rvert < 0.95$	$\lvert g^S_{RL}\rvert < 2.01$	$\lvert g^S_{LL}\rvert < 2.01$
$\lvert g^V_{RR}\rvert < 0.18$	$\lvert g^V_{LR}\rvert < 0.12$	$\lvert g^V_{RL}\rvert < 0.52$	$\lvert g^V_{LL}\rvert < 1.01$
$\lvert g^T_{RR}\rvert \equiv 0$	$\lvert g^T_{LR}\rvert < 0.08$	$\lvert g^T_{RL}\rvert < 0.51$	$\lvert g^T_{LL}\rvert \equiv 0$

29.2.3 Study of the Lorentz structure at *BES-III* [7]

Michel parameters

The coupling constants, $g^n_{\epsilon\omega}$ in Eq. 29.2.20, can be experimentally accessed via the energy spectra of the daughter leptons from tau decays. The polarization of the daughter leptons usually cannot be measured; however the polarization of the tau lepton P_τ in principle can be measured through its decay spectra. Under these assumptions the spectrum of the tau decays predicted by Eq. 29.2.20 can be parametrized at the Born level by the following sum of polynomials h_i:

$$\frac{1}{\Gamma}\frac{d\Gamma}{dx_\ell} = h_0(x_\ell) + \eta h_\eta(x_\ell) + \rho h_\rho(x_\ell) - P_\tau\left[\xi h_\xi(x_\ell) + \xi\delta h_{\xi\delta}(x_\ell)\right], \tag{29.2.22}$$

where P_τ is the average tau polarization and $x_\ell = E_\ell/E_{max}$ is the "reduced energy" of the daughter lepton, or the ratio of its energy to the maximum possible energy. Examples of the polynomials h_i are illustrated in Fig. 29.5.

The coefficients η, ρ, ξ, $\xi\delta$, known as the Michel parameters [51], are bilinear combinations of the coupling constants in Eq. 29.2.20. The four Michel parameters carry the full information on the coupling constants that can be extracted from the decay spectra of the tau leptons (without the measurement of the polarisation of the final state leptons).

In the Standard Model, the Michel parameters are predicted to be: $\rho = 0.75$; $\eta = 0$; $\xi = 1$; $\xi\delta = 0.75$. An observation of different values of the Michel parameters would indicate a violation of the Standard Model.

Anomalous tensor coupling

The parametrization presented in Eq. 29.2.20 is based on certain assumptions; namely it assumes the Hamiltonian to be lepton-number conserving, derivative-free, local, Lorentz invariant, and a 4-fermion point interaction. While most of these assumptions are quite

[7] By Igor R. Boyko. and Dedovich Dima

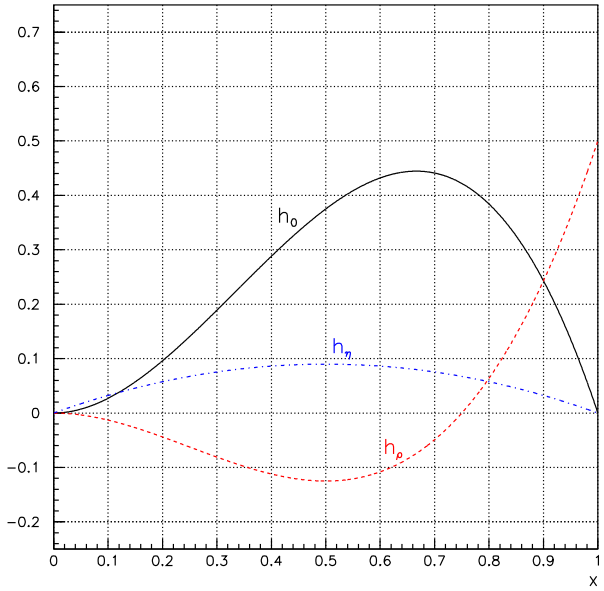

Figure 29.5: The shapes of polynomial functions h_i for the Michel parametrisation of tau decays.

natural, there is no fundamental reason to assume that the interaction Lagrangian does not include derivatives.

An anomalous interaction involving derivatives (which can only be a tensor interaction) can be represented in the following form [52]:

$$\mathcal{L} = \frac{g}{\sqrt{2}}\, W^{\alpha} \left\{ \overline{\tau}\gamma_{\alpha}\frac{1-\gamma^5}{2}\nu + \frac{\kappa_{\tau}^{W}}{2m_{\tau}}\partial_{\beta}\left(\overline{\tau}\sigma_{\alpha\beta}\frac{1-\gamma^5}{2}\nu\right)\right\} + \text{h.}c., \tag{29.2.23}$$

where κ_{τ}^{W} is the strength of the anomalous coupling. Such an anomalous interaction can be studied through the possible distortions of the energy spectra of tau decays. Since the Lagrangian of Eq. 29.2.23 explicitly contains derivatives, the distortions of the energy spectra can not be described in terms of the known Michel parameters.

The matrix element for the purely leptonic tau decays then takes the form:

$$\mathcal{M} = \frac{4G}{\sqrt{2}}\langle\overline{v}_l \mid \gamma_{\alpha}\mid v_{\overline{\nu}_l}\rangle \left(\langle\overline{v}_{\nu_\tau} \mid \gamma_{\alpha}\mid u_{\tau_L}\rangle - i\frac{\kappa_{\tau}^{W}}{2m_{\tau}}q_{\beta}\langle\overline{v}_{\nu_\tau} \mid \sigma_{\alpha\beta}\mid u_{\tau_R}\rangle\right), \tag{29.2.24}$$

where q is the four-momentum of the W. The first summand in Eq. 29.2.24 is the Standard Model prediction, while the second one is the contribution of the anomalous coupling. (In the framework of the Standard Model $\kappa_{\tau}^{W} = 0$.) In principle, both the anomalous coupling κ_{τ}^{W} and the "standard" couplings g_{ij}^{γ} can take non-Standard Model values simultaneously. In this case the first summand in (29.2.24) has to be replaced by the full parametrisation of Eq. 29.2.20.

Like the case of Michel parameters, the contribution of the anomalous tensor coupling can be also parametrized in terms of the polynomials. The approximate shape of the

energy spectrum is

$$\frac{1}{\Gamma}\frac{d\Gamma}{dx_\ell} \sim x_\ell^2 \cdot \left(-2x_\ell + 3 + 2 \cdot \kappa_\tau^W \cdot x_\ell\right). \tag{29.2.25}$$

Figure 29.6 compares the deviations of the decay spectrum from the Standard Model prediction for non-Standard Model values of κ_τ^W and the Michel parameter ρ. One can see that the change in shape is significantly different for the two cases, which makes it possible to measure the two parameters simultaneously.

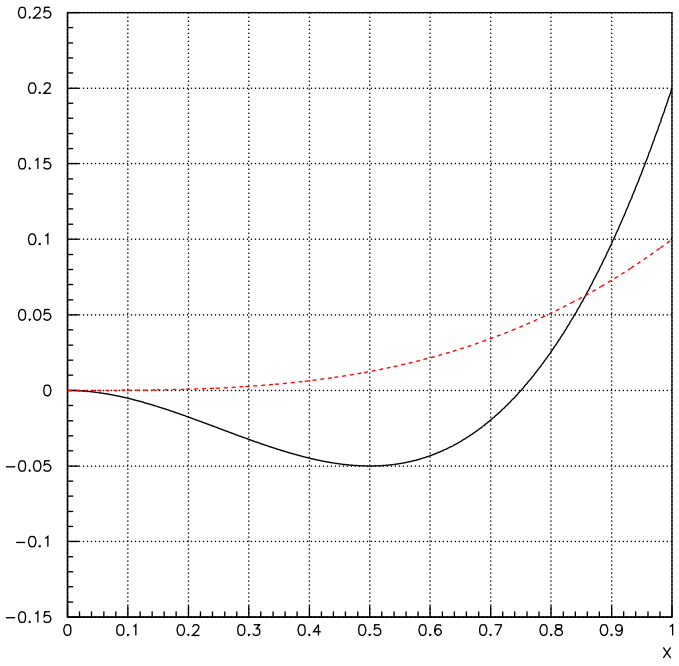

Figure 29.6: The deviation of the spectrum of leptons from tau decays from the Standard Model prediction. Dashed line: for the non-zero value of the anomalous tensor coupling. Solid line: for $\rho \neq 0.75$.

Measurement of Michel parameters and search for an anomalous tensor coupling

The Michel parameters have been extensively measured in tau lepton decays by many experiments. The current experimental uncertainty on the parameter ρ is about 0.008 and for η the uncertainty is 0.07 . To date, the anomalous tensor coupling has only been studied by the DELPHI experiment. The coupling constant κ_τ^W was measured with a precision of 0.04 and was found to be consistent with zero.

The *BES-III* experiment will have an abundant sample of tau lepton decays and an accurately measured energy spectrum. This will provide an excellent possibility to improve significantly the current knowledge on the Lorentz structure in tau decays. This section

presents a Monte-Carlo estimate of the possible reach of *BES-III* for measurements of the Michel parameters and in the search for the anomalous tensor coupling. For simplicity, only two Michel parameters ρ and η are considered.

The simulation was based on version 5.1 of the *BES-III* software. The events were generated at a c.m. energy of 3.69 GeV, where background from hadronic events is minimal. The following samples were simulated: 100K Bhabha scattering events $ee \to ee$; 20K dimuon events $ee \to \mu\mu$; 100K hadronic events $ee \to qq$. The total number of simulated tau pair events was 100K. The simulated signal was limited to the decay channel $ee \to \tau\tau \to e\mu$ (+neutrinos). This channel represents only about 3% of the total tau pairs, but these are rather easy events to select. The possible inclusion of hadronic tau decays can increase the available statistics significantly, therefore the results presented in this section can be considered as a conservative estimate of the *BES-III* reach.

The analysis was restricted to the angular region $|\cos\theta| < 0.83$. The event selection was based on the particle identification. Exactly two reconstructed charged particles were required in the event. One of them was required to be identified as an electron and the other had to be a muon. The main criterion for particle identification was based on the dE/dx pull variable, *i.e.* the deviation of the measured dE/dx value from the expected one, expressed in units of the dE/dx uncertainty. Figure 29.7 shows the pulls for the muon and electron hypotheses for the electron and muon candidates. One can see that the dimuon and Bhabha events are rejected very efficiently.

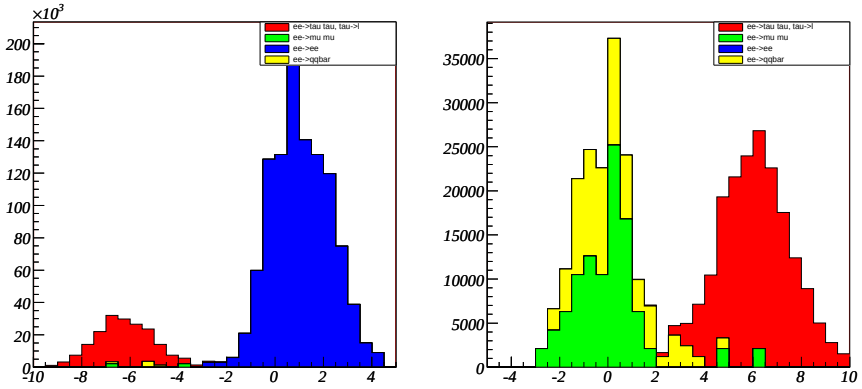

Figure 29.7: Left: the muon hypothesis pull for the electron candidate. Right: the electron hypothesis pull for the muon candidate. The selection cuts were +3 for the electron candidate and -3 for the muon candidate.

Several additional cuts were applied for further background suppression. The electron and muon candidates were required to be identified as such by the electromagnetic calorimeter (EMC) and muon chambers, respectively. Figure 29.8 illustrates the selection criteria. In addition, TOF information was used to reject protons and kaons from hadronic events in the momentum regions where dE/dx of these particles is close to that of electrons.

The signal selection efficiency was found to be about 30% (with respect to the full solid angle). For an integrated luminosity of 5 fb^{-1}, this efficiency corresponds to 180K

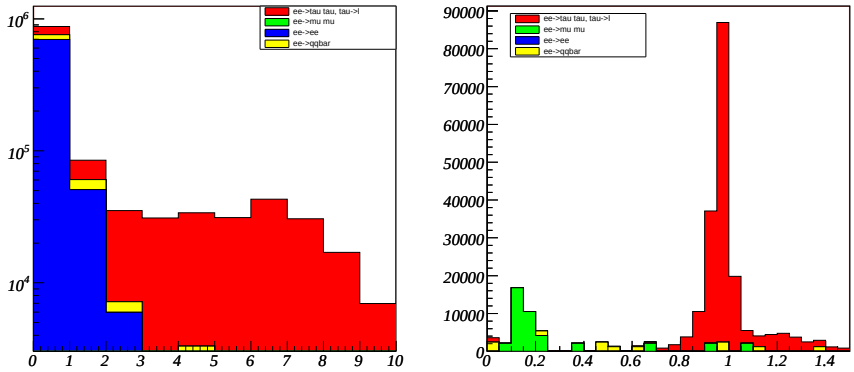

Figure 29.8: Left: the number of hits in muon chambers associated with the muon candidates. Right: the relative electromagnetic energy deposition E/P in the EMC for the electron candidates. The selection cuts were: $N_{HIT} \geq 3$ for muons and $E/P > 0.8$ for electrons.

selected signal events. The residual background is 6%, about half of which are hadronic events $ee \to qq$. The momentum spectra of the selected electron and muon candidates are presented in Fig. 29.9

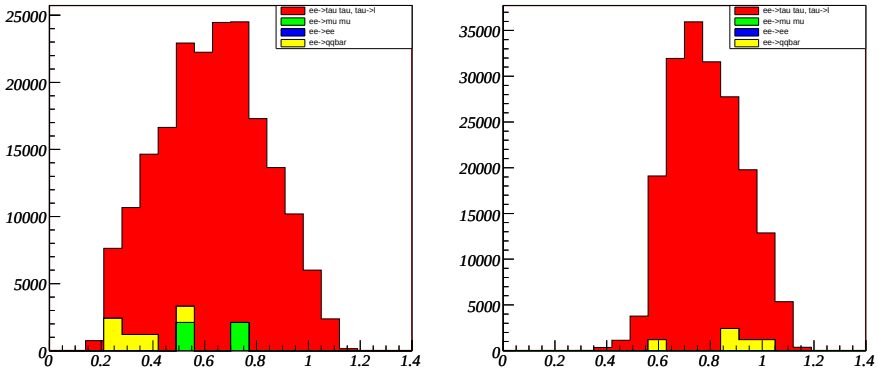

Figure 29.9: The momentum spectra of the selected muon (left) and electron (right) candidates. The statistics corresponds to a 5 fb^{-1} data sample.

The spectra of reconstructed momenta of electrons and muons from tau decays were fitted to the expectations for different values of the Michel parameter ρ and the anomalous coupling constant κ_τ^W. The statistical uncertainties of the fit parameters are:

$$\sigma(\rho) = 0.003$$

$$\sigma(\eta) = 0.02$$

$$\sigma(\kappa_\tau^W) = 0.002$$

The statistical errors correspond to a 5 fb^{-1} data sample collected at a c.m. energy of 3.69 GeV.

Summary

The *BES-III* experiment will provide excellent opportunities to study the Lorentz structure of tau decays, including the measurements of the Michel parameters and a search for an anomalous tensor coupling. Conservative estimates based on Monte-Carlo simulation of leptonic tau decays suggest that the current precision on the Michel parameters can be improved by factors of 2-4, and the limits on the anomalous coupling constant κ_τ^W can be improved by at least a factor of 10 with a 5 fb^{-1} data sample collected at $E_{cm} = 3.69$ GeV. The inclusion of hadronic tau decays into analysis would significantly improve the precision.

29.3 Semileptonic Decays[8]

29.3.1 Two-body Semileptonic Decays

The τ is the only known lepton massive enough to decay into hadrons. Its semileptonic decays are, thus, ideally suited for studying the hadronic weak currents in very clean conditions. The decay $\tau^- \to \nu_\tau H^-$ probes the matrix element of the left–handed charged current between the vacuum and the final hadronic state H^-.

For the decay modes with lowest multiplicity, $\tau^- \to \nu_\tau \pi^-$ and $\tau^- \to \nu_\tau K^-$, the relevant matrix elements (the so-called decay constants $f_{\pi,K}$) are already known from the measured decays $\pi^- \to \mu^- \bar{\nu}_\mu$ and $K^- \to \mu^- \bar{\nu}_\mu$. The corresponding τ decay widths can then be accurately predicted:

$$R_{\tau/\pi} \equiv \frac{\Gamma(\tau^- \to \nu_\tau \pi^-)}{\Gamma(\pi^- \to \mu^- \bar{\nu}_\mu)} = \left|\frac{g_\tau}{g_\mu}\right|^2 \frac{m_\tau^3}{2 m_\pi m_\mu^2} \frac{(1 - m_\pi^2/m_\tau^2)^2}{(1 - m_\mu^2/m_\pi^2)^2} \left(1 + \delta R_{\tau/\pi}\right), \qquad (29.3.26)$$

$$R_{\tau/K} \equiv \frac{\Gamma(\tau^- \to \nu_\tau K^-)}{\Gamma(K^- \to \mu^- \bar{\nu}_\mu)} = \left|\frac{g_\tau}{g_\mu}\right|^2 \frac{m_\tau^3}{2 m_K m_\mu^2} \frac{(1 - m_K^2/m_\tau^2)^2}{(1 - m_\mu^2/m_K^2)^2} \left(1 + \delta R_{\tau/K}\right). \qquad (29.3.27)$$

Owing to the different energy scales involved, the radiative corrections to the $\tau^- \to \nu_\tau \pi^-/K^-$ amplitudes are, however, not the same as the corresponding effects in $\pi^-/K^- \to \mu^- \bar{\nu}_\mu$. The relative corrections have been estimated [53, 54] to be:

$$\delta R_{\tau/\pi} = (0.16 \pm 0.14)\% \,, \qquad \delta R_{\tau/K} = (0.90 \pm 0.22)\% \,. \qquad (29.3.28)$$

Using these numbers, the measured $\tau^- \to \pi^- \nu_\tau$ and $\tau^- \to K^- \nu_\tau$ decay rates imply the $|g_\tau/g_\mu|$ ratios given in Table 29.1.

Assuming universality in the $W^\pm$ quark couplings, these decay modes determine the ratio [2, 33]

$$\frac{|V_{us}|\, f_K}{|V_{ud}|\, f_\pi} = \begin{cases} 0.27618 \pm 0.00048 & [\Gamma_{K/\pi \to \nu_\mu \mu}], \\ 0.267 \pm 0.005 & [\Gamma_{\tau \to \nu_\tau K/\pi}]. \end{cases} \qquad (29.3.29)$$

The very different accuracies reflect the present poor precision on $\Gamma(\tau^- \to \nu_\tau K^-)$. *BES-III* could considerably improve the measurements of the $\tau^- \to \nu_\tau K^-$ and $\tau^- \to \nu_\tau \pi^-$ branching ratios. The monochromatic kinematics of the final hadron at threshold will make possible a clean separation of each decay mode and, therefore, excellent accuracy.

29.3.2 Decays into Two Hadrons

For the two–pion final state, the hadronic matrix element is parameterized in terms of the so-called pion form factor $[s \equiv (p_{\pi^-} + p_{\pi^0})^2]$:

$$\langle \pi^- \pi^0 | \bar{d} \gamma^\mu u | 0 \rangle \equiv \sqrt{2}\, F_\pi(s)\, (p_{\pi^-} - p_{\pi^0})^\mu \,. \qquad (29.3.30)$$

A dynamical understanding of the pion form factor can be achieved [55, 56, 57, 58], using analyticity, unitarity and some general properties of QCD, such as chiral symmetry

[8] By A. Pich

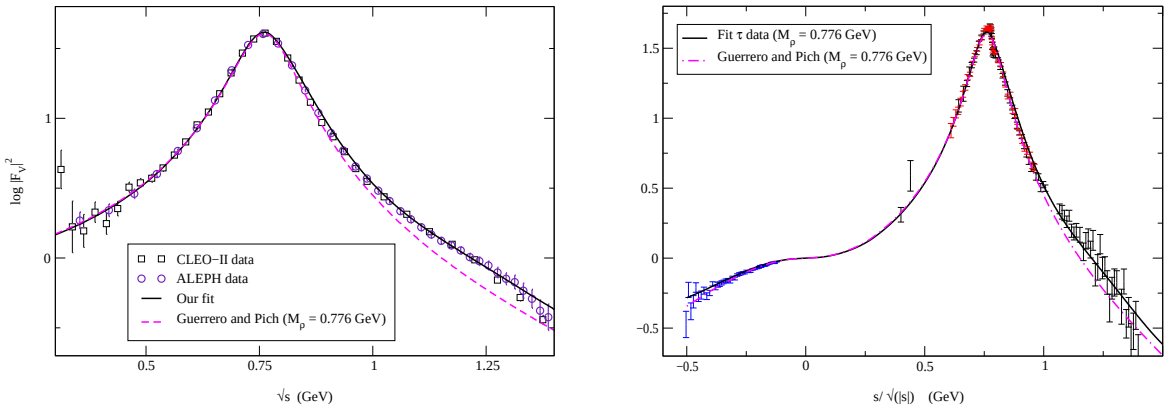

Figure 29.10: The pion form factor from τ data [62, 63] (left) and e^+e^- data [64, 65] (right), compared with theoretical predictions [55, 56]. The dashed lines correspond to the expression in Eq. 29.3.31.

[59] and the short-distance asymptotic behavior [60, 61]. Putting all these fundamental ingredients together, one gets the result [56]

$$F_\pi(s) = \frac{M_\rho^2}{M_\rho^2 - s - iM_\rho\Gamma_\rho(s)} \exp\left\{-\frac{s\,\mathrm{Re}A(s)}{96\pi^2 f_\pi^2}\right\}, \tag{29.3.31}$$

where

$$A(s) \equiv \log\left(\frac{m_\pi^2}{M_\rho^2}\right) + 8\frac{m_\pi^2}{s} - \frac{5}{3} + \sigma_\pi^3 \log\left(\frac{\sigma_\pi + 1}{\sigma_\pi - 1}\right) \tag{29.3.32}$$

contains the one-loop chiral logarithms, $\sigma_\pi \equiv \sqrt{1 - 4m_\pi^2/s}$ and the off-shell ρ width [56, 57] is given by $\Gamma_\rho(s) = \theta(s - 4m_\pi^2)\,\sigma_\pi^3\, M_\rho\, s/(96\pi f_\pi^2)$. This prediction, which only depends on M_ρ, m_π and the pion decay constant f_π, is compared with the data in Fig. 29.10. The agreement is rather impressive and extends to negative s values, where the $e^-\pi$ elastic data applies.

The small effects of heavier ρ resonance contributions and additional next-to-leading order $1/N_C$ corrections can be easily included, at the price of having some free parameters that decrease the predictive power [55, 58]. This gives a better description of the ρ' shoulder around 1.2 GeV (continuous lines in Fig. 29.10). A clear signal for the $\rho''(1700)$ resonance in $\tau^- \to \nu_\tau\pi^-\pi^0$ events has been reported by Belle (see Fig. 29.11), with a data sample 20 times larger than that of previous experiments [66].

The $\tau^- \to \nu_\tau\pi^-\pi^0$ decay amplitude can be related through an isospin rotation with the isovector piece of $e^+e^- \to \pi^+\pi^-$. Thus, for $s < m_\tau^2$, $F_\pi(s)$ can be obtained from the two sets of data. At present, there exists a serious discrepancy between e^+e^- and τ data. From e^+e^- data one predicts $\mathrm{Br}(\tau \to \nu_\tau 2\pi) = (24.48 \pm 0.18)\%$, which is $4.5\,\sigma$ smaller than the direct τ measurement $(25.40 \pm 0.10)\%$ [67]. This discrepancy translates into two different estimates of the hadronic vacuum polarization to the anomalous magnetic moment of the muon; while the e^+e^- data leads to a theoretical prediction for $(g-2)_\mu$ which is $3.3\,\sigma$ below the BNL-E821 measurement, the prediction obtained from the τ data is in much better agreement ($0.9\,\sigma$) with the experimental value [7].

Clearly, new precise e^+e^- and τ data sets are needed. The present experimental situation is very unsatisfactory, showing internal inconsistencies among different e^+e^-

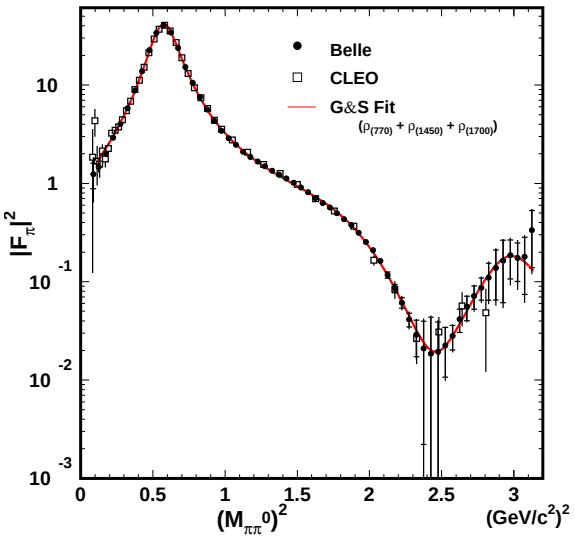

Figure 29.11: Preliminary Belle measurements of the pion form factor from $\tau^- \to \nu_\tau \pi^- \pi^0$ decays [66].

and τ measurements. The KLOE e^+e^- invariant-mass distribution does not agree with CMD2 and SND, while the most recent Belle measurement of the τ decay spectrum [66] slightly disagrees with ALEPH and CLEO [67]. The accurate measurement of $F_\pi(s)$ at *BES-III* could clarify this important issue.

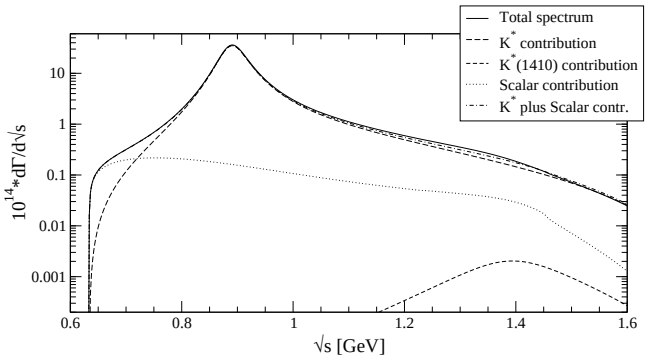

Figure 29.12: Predicted $\tau \to \nu_\tau K\pi$ distribution, together with the separate contributions from the $K^*(892)$ and $K^*(1410)$ vector mesons as well as the scalar component residing in $F_0^{K\pi}(s)$ [68].

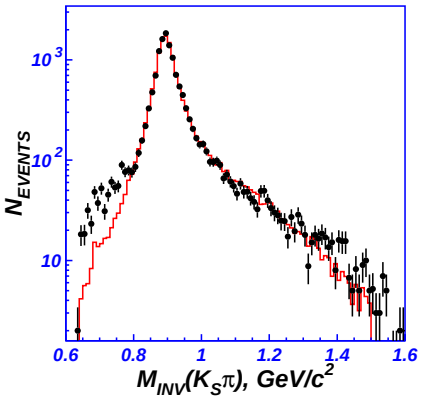

Figure 29.13: $K_S\pi$ invariant-mass distribution from BELLE $\tau \to \nu_\tau K_S\pi$ events. The histogram shows the expected $K^*(892)$ contribution [70].

More recently, the decay $\tau \to \nu_\tau K\pi$ has been studied in Ref. [68]. The hadronic spectrum, shown in Fig. 29.12, is characterized by two form factors,

$$\frac{d\Gamma_{K\pi}}{d\sqrt{s}} = \frac{G_F^2 |V_{us}|^2 m_\tau^3}{32\pi^3 s}\left(1-\frac{s}{m_\tau^2}\right)^2\left[\left(1+2\,\frac{s}{m_\tau^2}\right) q_{K\pi}^3 |F_+^{K\pi}(s)|^2 + \frac{3\Delta_{K\pi}^2}{4s}\, q_{K\pi} |F_0^{K\pi}(s)|^2\right], \tag{29.3.33}$$

where $q_{K\pi} = \frac{1}{2\sqrt{s}}\,\lambda^{1/2}(s, m_K^2, m_\pi^2)$ and $\Delta_{K\pi} = m_K^2 - m_\pi^2$. The vector form factor $F_+^{K\pi}(s)$

has been described in an analogous way to $F_\pi(s)$, while the scalar component $F_0^{K\pi}(s)$ takes into account additional information from $K\pi$ scattering data through dispersion relations [33, 69]. The decay width is dominated by the $K^*(892)$ contribution, with a predicted branching ratio $\mathrm{Br}[\tau \to \nu_\tau K^*] = (1.253 \pm 0.078)\%$, while the scalar component is found to be $\mathrm{Br}[\tau \to \nu_\tau (K\pi)_{\mathrm{S-wave}}] = (3.88 \pm 0.19) \cdot 10^{-4}$.

Preliminary measurements of the $\tau^- \to \nu_\tau K_S \pi^-$ (Belle [70]) and $\tau^- \to \nu_\tau K^- \pi^0$ (BaBar [71]) distributions show clear evidence for the scalar contribution at low invariant masses and a $K^*(1410)$ vector component at large s (see Fig. 29.13).

The dynamical structure of other hadronic final states can be investigated in a similar way. The $\tau \to \nu_\tau 3\pi$ decay mode was studied in Ref. [72], where a theoretical description of the measured structure functions [73, 74, 16] was provided. A detailed analysis of other τ decay modes into three final pseudoscalar mesons is in progress [75]. The more complicated $\tau \to \nu_\tau 4\pi$ and $e^+e^- \to 4\pi$ transitions have also been studied [76]. Accurate experimental measurements of the hadronic decay distributions would provide a very valuable data set to perform important tests of QCD in the non-perturbative regime. Violation in τ

29.4 Search for CP Violation in τ decays[9]

There are two powerful motivations for probing *CP* symmetry in lepton decays:

- The discovery of *CP* asymmetries in B decays that are close to 100 % in a sense 'de-mystifies' *CP* violation, in that it established that complex *CP* phases are not intrinsically small and can even be close to 90 degrees. This de-mystification would be completed, if *CP* violation were found in the decays of leptons as well.

- We know that CKM dynamics, which is so successful in describing quark flavour transitions, is utterly irrelevant to baryogenesis. There are actually intriguing arguments for baryogenesis being merely a secondary effect driven by primary leptogenesis [77]. To make the latter less speculative, one has to find *CP* violation in leptodynamics.

The strength of these motivations has been well recognized in the community, as can be seen from the planned experiments to measure *CP* violation in neutrino oscillations and the ongoing heroic efforts to find an electron EDM. Yet there are other avenues to this goal as well that certainly are at least as challenging, namely to probe *CP* symmetry in τ decays. There is also a less orthodox probe, namely attempting to extract an EDM for τ leptons from $e^+e^- \to \tau^+\tau^-$. It is understood that the Standard Model does not produce an observable effect here. One should also note that one is searching for a *CP*-odd effect in an *electromagnetic* production process unlike in τ decays, which are controlled by the weak force.

The betting line is that τ decays – next to the electron EDM and ν oscillations – provide the best stage to search for manifestations of *CP* breaking leptodynamics. There exists a considerable literature on the subject started by discussions on a tau-charm factory more than a decade ago [78, 79, 80, 81], which has recently attracted renewed interest recently [82, 83, 84, 85] especially stressing the following points:

[9] By I. I. Bigi

- There are many more decay channels for tau lepons than for muons, making the constraints imposed by CPT symmetry much less restrictive.

- The τ lepton has sizable rates into multibody final states. Due to their nontrivial kinematics, asymmetries can emerge in the final-state distributions, where they are likely to be significantly larger than in the integrated widths. The channel

$$K_L \to \pi^+\pi^- e^+ e^-$$

  illustrates this point. It commands only the tiny branching ratio of $3 \cdot 10^{-7}$. The forward-backward asymmetry $\langle A \rangle$ in the angle between the $\pi^+\pi^-$ and e^+e^- planes constitutes a CP-odd observable. It has been measured by KTeV and NA48 to be truly large, namely about 13 %, although it is driven by the small value of $|\epsilon_K| \sim 0.002$. One can, thus, trade branching ratio for the size of a CP asymmetry.

- New Physics in the form of multi-Higgs models can contribute on the tree-level, such as the SM W exchange.

- Some of the channels could exhibit enhanced sensitivity to New Physics.

- Having polarized τ leptons provides a powerful handle on CP asymmetries as well as control over systematics.

These features will be explained in more detail below. It seems clear that such measurements can be performed only in e^+e^- annihilation, *i.e.* at *BES-III*, the existing B factories, or better still at a Super-Flavour factory. There one has the added advantage that one can realistically obtain highly polarized τ leptons: This can be achieved directly by having the electron beam longitudinally polarized or more indirectly even with unpolarized beams by using the spin alignment of the produced τ pair to 'tag' the spin of the τ under study by the decay of the other τ like $\tau \to \nu\rho$.

29.4.1 $\tau \to \nu K \pi$

The most promising channels for exhibiting CP asymmetries are $\tau^- \to \nu K_S \pi^-$, $\nu K^- \pi^0$ [81]:

- Due to the heaviness of the lepton and quark flavours they are most sensitive to nonminimal Higgs dynamics while being Cabibbo suppressed in the SM.

- They can show asymmetries in the final state distributions.

The SM does generate a CP asymmetry in τ decays that should be observable. Based on known physics one can reliably predict a CP asymmetry [82]:

$$\frac{\Gamma(\tau^+ \to K_S \pi^+ \overline{\nu}) - \Gamma(\tau^- \to K_S \pi^- \nu)}{\Gamma(\tau^+ \to K_S \pi^+ \overline{\nu}) + \Gamma(\tau^- \to K_S \pi^- \nu)} = (3.27 \pm 0.12) \times 10^{-3} \tag{29.4.34}$$

due to K_S's preference for antimatter over matter. Strictly speaking, this prediction is more general than the SM: no matter what produces the CP impurity in the K_S wave

function, the effect underlying Eq. 29.4.34 has to be present, while of course not affecting $\tau^{\mp} \to \nu K^{\mp}\pi^0$.

To generate a *CP* asymmetry, one needs two different amplitudes that contribute coherently. This requirement is satisfied, since the $K\pi$ system can be produced from the (QCD) vacuum in a vector and scalar configuration with form factors F_V and F_S, respectively. Both are present in the data, with the vector component (mainly in the form of the K^*) dominant as expected [6]. Within the SM, there is no weak phase between them at any observable level, yet it can readily be provided by a charged Higgs exchange in non-minimal Higgs models, which contribute to F_S.

A few general remarks on the phenomenology might be helpful to set the stage. For a *CP* violation in the underlying weak dynamics to generate an observable asymmetry in partial widths or energy distributions, one also needs a relative strong phase between the two amplitudes:

$$\Gamma(\tau^- \to \nu K^-\pi^0) - \Gamma(\tau^+ \to \bar{\nu} K^+\pi^0), \frac{d}{dE_K}\Gamma(\tau^- \to \nu K^-\pi^0) - \frac{d}{dE_K}\Gamma(\tau^+ \to \bar{\nu} K^+\pi^0) \propto \mathrm{Im}(F_H F_V^*)\mathrm{Im} g_H g_W^* \ , \tag{29.4.35}$$

where F_H denotes the Higgs contribution to F_S and g_H its weak coupling. This should not represent a serious restriction, since the $K\pi$ system is produced in a mass range with several resonances. If, on the other hand, one is searching for a T-odd correlation such as

$$O_T \equiv \langle \vec{\sigma}_\tau \cdot (\vec{p}_K \times \vec{p}_\pi) \rangle \ , \tag{29.4.36}$$

then *CP* violation can surface even with*out* a relative strong phase

$$O_T \propto \mathrm{Re}(F_H F_V^*)\mathrm{Im} g_H g_W^* \ . \tag{29.4.37}$$

However, there is a caveat: final state interactions can generate T-odd moments even from T-invariant dynamics, where one has

$$O_T \propto \mathrm{Im}(F_H F_V^*)\mathrm{Re} g_H g_W^* \ . \tag{29.4.38}$$

Fortunately one can differentiate between the two scenarios of Eqs. 29.4.37 and 29.4.38 at *BES-III* by comparing directly the T-odd moments for the *CP*-conjugate pair τ^+ and τ^-:

$$O_T(\tau^+) \neq O_T(\tau^-) \quad \Longrightarrow \quad CP \text{ violation!} \tag{29.4.39}$$

A few numerical scenarios might illuminate the situation: a Higgs amplitude 1% or 0.1% the strength of the SM W-exchange amplitude – the former [latter] contributing [mainly] to F_S [F_V] – is safely in the 'noise' of present measurements of partial widths; yet it could conceivably create a *CP* asymmetry as large 1% or 0.1%, respectively. More generally a *CP*-odd observable in a SM allowed process is merely *linear* in a New Physics amplitude, since the SM provides the other amplitude. On the other hand SM-forbidden transitions – say lepton-flavour violation as in $\tau \to \mu\gamma$ – have to be *quadratic* in the New Physics amplitude.

$$CP - \text{odd} \propto |T_{SM}^* T_{NP}| \ \text{ vs. } \ \text{LFV} \propto |T_{NP}|^2 \tag{29.4.40}$$

Probing *CP* symmetry on the 0.1% level in $\tau \to \nu K\pi$ thus has roughly the same sensitivity for a New Physics amplitude as searching for $\mathrm{BR}(\tau \to \mu\gamma)$ on the 10^{-8} level.

CLEO has undertaken a pioneering search for a *CP* asymmetry in the angular distribution of $\tau \to \nu K_S\pi$ placing an upper bound of a few percent [86].

29.4.2 Other τ decay modes

It appears unlikely that analogous asymmetries could be observed in the Cabibbo allowed channel $\tau \to \nu\pi\pi$, yet detailed studies of $\tau\nu 3\pi/4\pi$ look promising, also because the more complex final state allows one to form T-odd correlations with unpolarized τ leptons; on the other hand, decays of polarized τ leptons might exhibit much larger CP asymmetries [83].

Particular attention should be paid to $\tau \to \nu K 2\pi$, which has potentially very significant additional advantages:
$\oplus$: One can interfere *vector* with *axial vector* $K2\pi$ configurations.
$\oplus$: The larger number of kinematical variables and of specific channels should provide more internal cross checks of systematic uncertainties such as detection efficiencies for positive vs. negative particles.